Egyptian Journal of Chemistry
http://ejchem.journals.ekb.eg/

# Structural, Electronic, Optical Properties and Molecular Dynamics Study of $WO_3$ $W_{0.97}Ag_{0.03}O_3$ and $W_{0.94}Ag_{0.06}O_3$ Photocatalyst by the First Principle of DFT Study

**Abdullah Al Mamun[a], Monsur Alam[a], Ahsan Habib[b,c], Unesco Chakma[d]*, M.A. Mokit Sikder[a] and Ajoy Kumer[e,f]***

[a]*Department of Civil Engineering, European University of Bangladesh, Gabtoli, Dhaka-1216, Bangladesh*

[b]*Division of Building Material, Housing and Building Research Institute, 120/3, Darussalam, Mirpur Road, Dhaka 1216*

[c]*Department of Chemical Engineering and Polymer Science, Shahjalal University of Science and Technology, Sylhet-3114, Bangladesh*

[d]*Department of Electrical and Electronics Engineering, European University of Bangladesh, Gabtoli, Dhaka-1216, Bangladesh*

[e]*Department of Chemistry, European University of Bangladesh, Gabtoli, Dhaka-1216, Bangladesh*

[f]*Department of Chemistry, Bangladesh University of Engineering and Technology, Dhaka-1000, Bangladesh*

**Abstract**

This study examined the theoretical impact and modeling of photocatalyst, WO3, on organic pollutants and wastewater treatment. The electronic band structures, total density of state, all -optical properties, and photocatalytic activities under UV or visible light were investigated by using the first principle method for WO3 and Ag-doped by 3% and 6%. In order to calculate band gap, generalized gradient approximation (GGA) based on Perdew- Burke- Ernzerhof (PBE) was used. The band gap for WO3 was found 2.03eV. To recognize the character of photocatalyst activities, the optical properties were investigated and calculated. For obtaining better value in band gap, 3% and 6% Ag were doped; found 0.227eV and 0.171 eV, respectively. Concurrently, optical properties, absorption, reflection, refractive index, conductivity, dielectric function, and loss function were calculated. Having doped Ag with WO3, the optical properties had changed and improved the photocatalytic effect to the hybridization of 4s, 3d, and 4p orbitals of Ag. From the value of band gap and optical properties, it is clear that W0.97Ag0.03O3 and W0.94Ag0.06O3 can provide better conductivity rather than WO3.

Keywords: Photocatalyst, Electronic structure, DOS, PDOS and optical properties.

## 1. Introduction

Water contamination with multifarious organic pollutants is being regarded as one of the most lethal problems facing living beings, leading to cause esthetic pollution, eutrophication, and perturbation to aquatic life cycle as well [1; 2; 3]. In order to address this existing and serious crisis, many researches- laboratory works, thesis works–have been studied. In recent years, sunlight-driven semiconductor photocatalysis is considered to be a pragmatic and cost-effective approach to focus on existing water issues [4; 5; 6; 7; 8]. Photocatalysis is a green and eco-friendly method to address the pollution of wastewater owing to its merits of high efficiency, chemical stability, having good adsorption, low synthesis cost, and non-toxicity[9; 10; 11; 12]. It has been provided that Sunlight or UV light in the solar spectrum which occupies,

*Corresponding author e-mail: Ajoy Kumer, kumarajoy.cu@gmail.com; Orcid: 0000-0001-5136-6166, Research ID: AAM-4654-2020 and Cell: 01770568699: and Unesco Chakma; unescochakma@gmail.com
Receive Date: 07 March 2021, Revise Date: 16 April 2021, Accept Date: 01 May 2021
DOI: 10.21608/EJCHEM.2021.66630.3433

generally, 4-5% of energy, though it may vary based on water quality [13; 14; 15]. A huge number of photocatalyst with photocatalytic and antibacterial properties, chemical properties, and some other catalysts have been reported in which UV light works vary [16; 17; 18; 19; 20; 21; 22; 23; 24; 25; 26]. Among several semiconductor materials, $WO_3$, an efficient, photochemical stable, nonhazardous photocatalyst - has been taken comprehensively in our research in order to address water pollution [27; 28; 29; 30]. As a photocatalyst, tungsten oxide ($WO_3$) nonmaterial has good photocatalytic performance and chemical stability in the process of catalytic reaction [30; 31; 32; 33]. Therefore, this is one of the widely used and studied photocatalysts in wastewater treatment. Even its application in catalysis is limited because of its wide band gap (2.03eV). In the research, silver (Ag) had been doped with tungsten oxide ($WO_3$) owing to mitigate band gap and develop efficiency. In doping technology or as a catalyst, tungsten oxide ($WO_3$) has striking properties and features [34]. As the doping density (3%, 6%) rises, the width of the impurity band within the gap is broadened and merges with the conduction band (CB). As a result, the electrons are delocalized, as proven by the magnetic susceptibility and conductivity - they generally tend to become almost temperature-independent.

In continuation, this research covers the recent study of tungsten oxide ($WO_3$), including the detailed and cleared data of electronic structure, nature of orbital, impact on the environment, impact on wastewater treatment, and optical properties.

## 2. Computational Methods

The theoretical calculations of tungsten oxide ($WO_3$), a semiconductor, were simulated by using the first-principles method and supercell approach. In the following figures 1(a), 1(b), and 1(c), the unit cell of $WO_3$, $W_{0.97}Ag_{0.03}O_3$, and $W_{0.94}Ag_{0.06}O_3$ in the cubic symmetry and 2×1×1 supercell model considered. These model- structures of $WO_3$, $W_{0.97}Ag_{0.03}O_3$, and $W_{0.94}Ag_{0.06}O_3$ were made using 33 atoms, 84 atoms of oxygen, 28 atoms of Tungsten. All of the calculations in this study relating to wastewater treatment were conducted by material studio 8.0, multitasking software. In order to calculate the band gap or band structure, the total density of state, and partial density of state, GGA method with PBE was used. These were the optimization of CASTEP code [35; 36] from material studio 8.0 as well [37].

## 3. Results and discussion

### *3.1. Optimized structure*

Having completed Geometry optimization, the lattice parameter values have been calculated for the crystal. The values are: a= 7.301098 Å, b= 7.449006 Å, c= 10.243191 Å. Angles among them have also been measured. These are: $\alpha = 90.13587^0$ $\beta = 93.004233^0$, $\gamma = 93.502035^0$. Tungsten oxide ($WO_3$) crystal is a monoclinic crystal. The space group is Harmanna Mauguin $P\bar{1}$, triclinic crystal system, point group, hall $P\bar{1}$, density 4.85 g/cm$^3$ shown in figure 1(a). The Ag-doped optimized structures are accounted in figure 1(b), and 1(c), where the same geometry is explained aptly.

### *3.2. Thermo Physical Properties*

The thermophysical properties, such as enthalpy, entropy, the heat of formation, heat capacity, and total or internal energy, are considered as the most important parameter for crystals as their uses. It is a very well known problem that the formation energy or heat of formation of tested alloys is not calculated the experimental value that is why for method validation, the crystal $Ag_3PO_4$ was simulated through the methods and GGA with PBE, which shows the close value to experimental value showing in table 1. The main cause for the selection of $Ag_3PO_4$ crystal is noted that it has experimental value. In the case of the alloy or crystals of condensed matter, the formation energy indicates the stability of the crystal. From table 1, the formation energies of $WO_3$, $W_{0.97}Ag_{0.03}O_3$, and $W_{0.94}Ag_{0.06}O_3$ are 170.67, 66.92, and 64.82 kcal/mol.

### *3.3. Surface area*

It was reported that the peak photocatalytic activity is directed related to the specific surface area of photocatalyst, and this value is different for different series at variable pH value. So that higher value of surface area indicated the higher photocatalytic activity of catalyst [39]. In figure 2, there are listed the surface area for calculation of theoretical investigation of $WO_3$, $W_{0.97}Ag_{0.03}O_3$, and $W_{0.94}Ag_{0.06}O_3$ crystal, and one point is noted for that doping process has performed with constant surface area for all crystals.

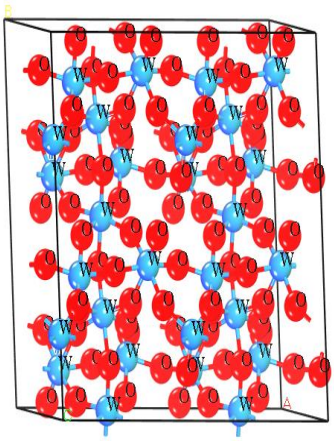

**Figure 1**(a): Structure for $WO_3$

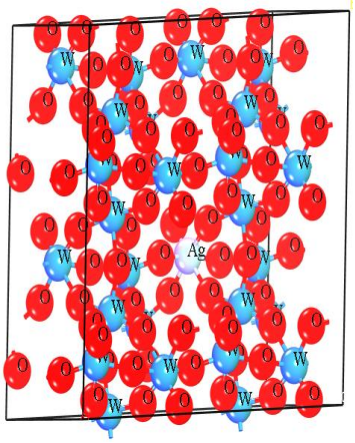

**Figure 1**(b): Structure for $W_{0.97}Ag_{0.03}O_3$

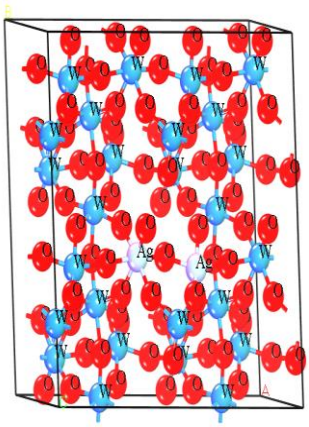

**Figure 1**(c): Structure for $W_{0.94}Ag_{0.06}O_3$

Table 1: Magnitude of formation energy for $WO_3$, $W_{0.97}Ag_{0.03}O_3$, and $W_{0.94}Ag_{0.06}O_3$

| Structure | Formation energy, kcal/mol | Experimental data kcal/mol |
|---|---|---|
| Ref. structure $Ag_3PO_4$ | 237.14 | 240.20 [38] |
| $WO_3$ | 170.67 | New predicted |
| $W_{0.97}Ag_{0.03}O_3$ | 66.92 | New predicted |
| $W_{0.94}Ag_{0.06}O_3$ | 64.82 | New predicted |

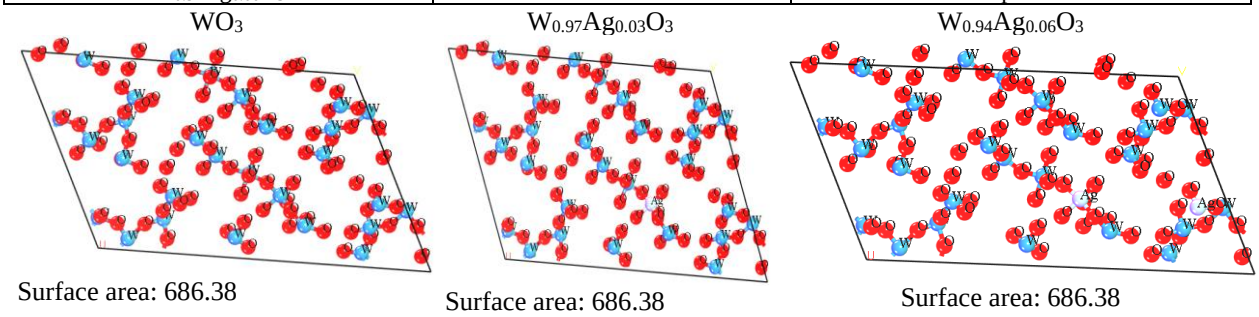


Figure 2: Surface area for $WO_3$, $W_{0.97}Ag_{0.03}O_3$, and $W_{0.94}Ag_{0.06}O_3$ crystals

### *3.4. Electronic Structure*

In order to determine the electronic band structure of $WO_3$, $W_{0.97}Ag_{0.03}O_3$, and $W_{0.94}Ag_{0.06}O_3$, the Fermi energy level was set at zero. As shown in figure 3(a), it was found that the minimum of conduction bands (MCB) was obtained within the G symmetry point, whereas the maximum of valance band (MVB) was ostensibly connected additionally in G symmetry points where each of MCB and MVB is joined, so that it is known as direct band gap. From figure 3(a), the calculated band gap has shown 2.03eV for $WO_3$. Having doped 3% of Ag – $W_{0.97}Ag_{0.03}O_3$—the band gap decreased magnificently, which has been recorded at 0.227 eV. The premier and interesting fact are that when 6% of Ag is doped, the band gap dramatically goes down and settled down at 0.171eV. To elucidate congruously the comparison, a table has been given along with the electronic structures.

### *3.5. Density of states and partial density of state*

The density of the state shows the character of electronic band structures and the splitting of an orbital. The density of states (DOS) of $WO_3$, Ag, and o atoms of $W_{0.97}Ag_{0.03}O_3$ and $W_{0.94}Ag_{0.06}O_3$ crystal were calculated by GGA with PBE functional. As shown in figure 4 (a), the valence bands square were occupied by consisting orbital including both of conduction band and valance band. From the figure 3(a), it has identified a noticeable change in the sum of DOS for $WO_3$, $W_{0.97}Ag_{0.03}O_3$, and $W_{0.94}Ag_{0.06}O_3$ crystals. Moreover, the figure 4(b), figure 4(c) represent the contribution of each atom in DOS, which

has mention as PDOS, and after doping the Fe atom, there has a vast upward trend in both of valance band and conduction band which could be considered as the reason of decreasing the band gap.

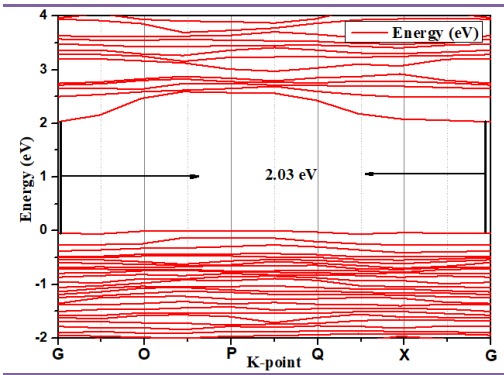


Figure 3(a): Electronic structure for $WO_3$

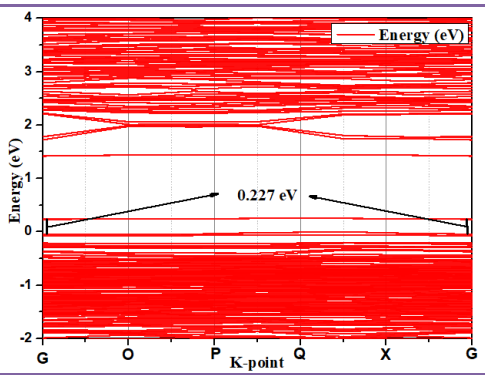


Figure 3(b): Electronic structure for $W_{0.97}Ag_{0.03}O_3$

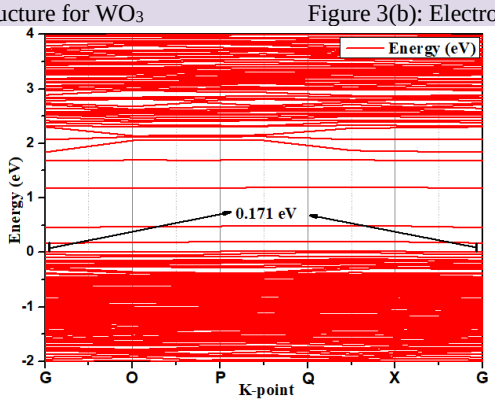


Figure 3 (c): $W_{0.94}Ag_{0.06}O_3$

Table 2: Band gap for $WO_3$ $W_{0.97}Ag_{0.03}O_3$ and $W_{0.94}Ag_{0.06}O_3$

| Sample | GGA with PBE | Experimental data |
|---|---|---|
| $WO_3$ | 2.031 eV | No data available |
| $W_{0.97}Ag_{0.03}O_3$ | 0.227 eV | New predicted |
| $W_{0.94}Ag_{0.06}O_3$ | 0.171 eV | New predicted |

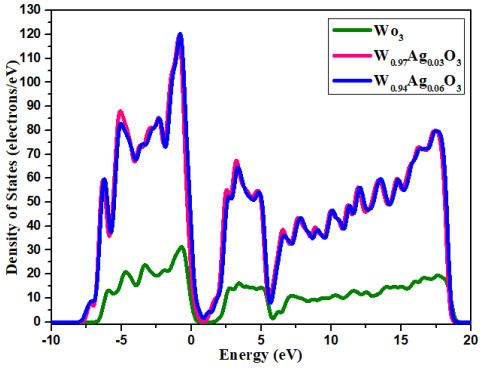


Figure 4(a): Comparison of the sum of DOS for doped and undoped $WO_3$

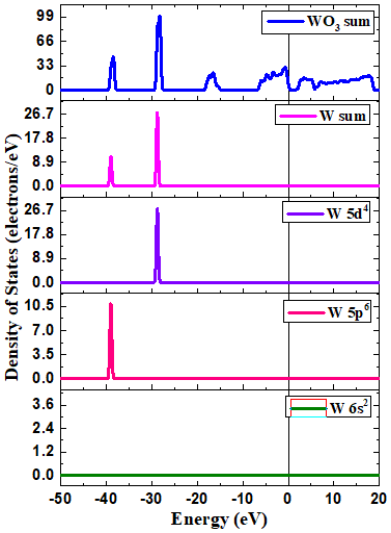


Figure 4(b): PDOS in $WO_3$ for W atom

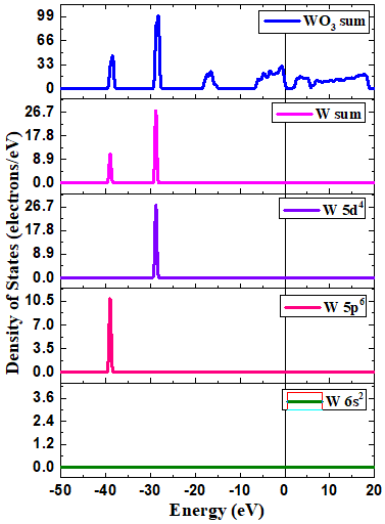


Figure 4(c): PDOS in $W_{0.97}Ag_{0.03}O_3$for W atom

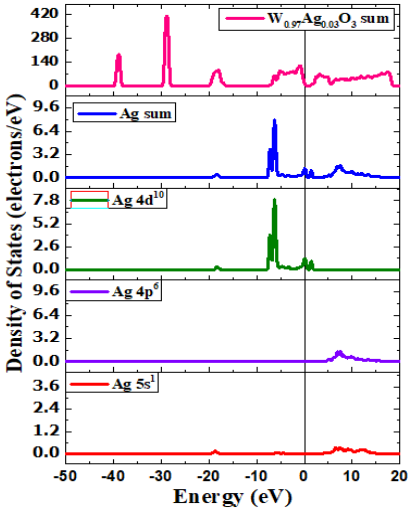


Figure 4(d): PDOS in $W_{0.97}Ag_{0.03}O_3$ Ag atom

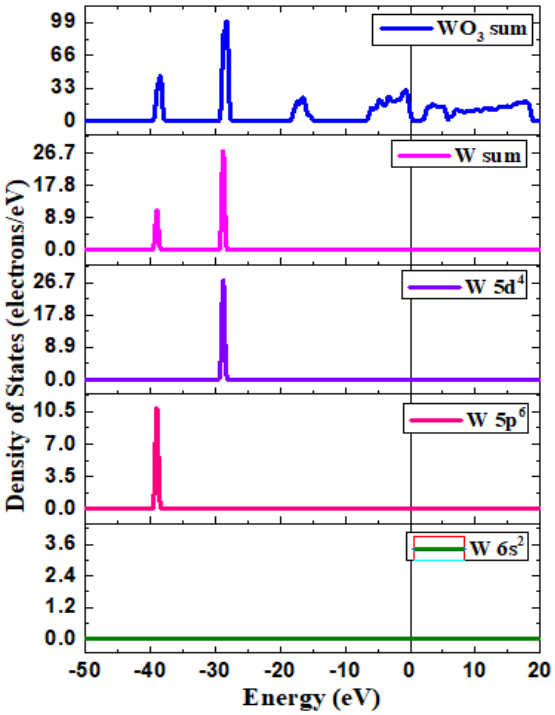


Figure 4(e): PDOS in $W_{0.94}Ag_{0.06}O_3$for W atom

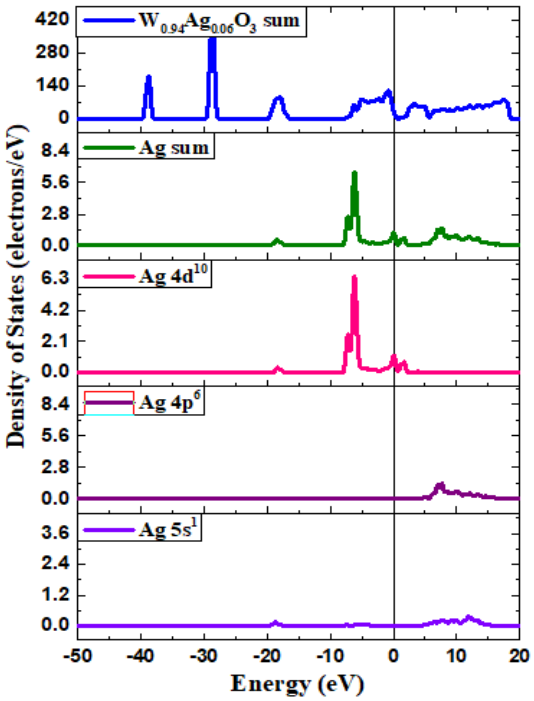


Figure 4(f): PDOS in $W_{0.94}Ag_{0.06}O_3$for Ag atom

### *3.6. Photo-catalyst activity*

Tungsten oxide ($WO_3$) is an n-type semiconductor material with a band gap between 2.7-2.8 eV. It has been using for ages for virus inactivation, energy conversion, and degradation of harmful pollutants from liquids –water. In visible light or UV light, Tungsten oxide ($WO_3$), a photo-catalyst, works and reacts exceedingly well. It has been proved that Tungsten oxide ($WO_3$) shows a considerable photo-absorption rate with UV or visible light. Photo-catalyst activity under visible light irradiation might be enhanced by morphology control, certain element of doping Ag atom. The change of energy band gaps happens when 3% of Ag and 6% of Ag is added with the Tungsten oxide ($WO_3$), which has been shown above. In the ruin of pollutants in liquid phase applications, this technique in which the powder of $WO_3$ is disseminated into a liquid pollutant

### *3.7. Optical properties*

#### *3.7.1. Optical reflectivity*

Reflectivity is an optical property of the material in which how much light is reflected from the material in relation to an amount of light incident on the material is defined. In our investigation, we determined the Reflectivity of $WO_3$, $W_{0.97}Ag_{0.03}O_3$, and $W_{0.94}Ag_{0.06}O_3$. We found that the initial frequency recorded was around 0.35 and 5.57 for $WO_3$. Once an ordered increase, it reached a decreasing of 0.15 at 15 units and abruptly accrued at 0.22. It dropped significantly concerning 0.02 at 23eV, which has been mentioned and shown in the figures. During the study of $W_{0.97}Ag_{0.03}O_3$ and $W_{0.94}Ag_{0.06}O_3$ Reflectivity, these were modified at the same point though these two were smaller than $WO_3$. Having investigated, we experienced a dramatic zigzag between 0 to 12 eV.

#### *3.7.2. Absorption*

In order to calculate and determine the optical absorption of $WO_3$, $W_{0.97}Ag_{0.03}O_3$, and $W_{0.94}Ag_{0.06}O_3$ materials, the polycrystalline polarization technique, the electrical field vector as an isotropic average were used. During the simulation, a small smearing value of 1.5 eV was applied to obtain additional distinguishable absorption peaks. The gained absorption peaks, which have been presented in the figure, were attributed to the image transition energies from the MVB to the MCB under visible light irradiation. These materials can absorb photons of visible range each of $WO_3$, $W_{0.97}Ag_{0.03}O_3$, and $W_{0.94}Ag_{0.06}O_3$ displays the modification at a similar point. $W_{0.97}Ag_{0.03}O_3$ and $W_{0.94}Ag_{0.06}O_3$ are slightly higher than $WO_3$.

#### *3.7.3. Refractive Index*

Refractive index or index of refraction is a value calculated as the ratio of the speed of light in a vacuum to that in another—second— medium of greater density. It is also used during the measurement of the concentration of a solute in an aqueous solution. In this research, a refractive index has been used for chemical degradation from the solution. The large value of the index of refraction related to the larger and denser medium. Figure 7 indicates the refraction index as a function of photon energy wherever the real part is and therefore, the imaginary part of a complex number for each of the doped and undoped mentioned has been showing an inverse pattern. At the very early stage of photon energy, the refraction index is higher for the real part while the imaginary part of a complex number is almost near to zero. Next, a decline of each and every element encounters them to each other for doped and undoped. Then they follow a constant pattern with outright different values of refraction index and the similar for every undoped and doped of $WO_3$.

#### *3.7.4. Dielectric function*

Owing to analyze the optical properties that are illustrated with sorption properties, the dielectric function tool is used; the following equation for solid is followed in this stage:

$$\varepsilon = \varepsilon_1(\omega) + i\varepsilon_2(\omega).$$

Here, $\varepsilon$ ($\omega$), and $\varepsilon_1$ ($\omega$) denote nonconductor constant—real part and the dielectric loss factor — imaginary part. Nonconductor function combines amity with the space of materials, which are physically the same as the permittivity or absolute permittivity. The real part of the dielectric function shows the energy storing capacity in the electric field and also represents the pure imaginary number of the energy dissipation capability of nonconductor materials. Figure 8 indicates that the imaginary part-number is a smaller amount than the real part from 0 eV to 5eV frequencies. However, the imaginary part becomes larger than the real part in between 6eV to 16eV and it indicates the same real and imaginary part for the doped and undoped $WO_3$

#### *3.7.5. Loss function*

For optical properties, there are two regions for the electronic energy function high energy function and low energy function. The higher loss function shows the higher energy region with modification of frequency or ranges. The opposite is the low energy loss function, which together with energy less than one, will provide data of composition and electronic structure. The energy loss function for optical properties is joined to the insulator constant of the materials. According to figure 9, the loss functions for $W_{0.97}Ag_{0.03}O_3$ and $W_{0.94}Ag_{0.06}O_3$ are higher than $WO_3$.

### *3.8. Molecular Dynamics*

Free energy may also be expressed in terms of averages over ensembles of molecular configurations for the molecular system with the vibrational modes, indicating the molecular stability through a multifarious system. From the total energy, it can be said that after doping the Ag atom in crystal, the total energy can be shifted four times from its initial states, which stands for the instability of molecular stage of doped crystal and give strong supports to the lowering electronic structure and variation of DOS, as well as PDOS. On the other hand, the kinetic energy and potential energy are related to the total energy, which is represented in the following figures and their distribution.

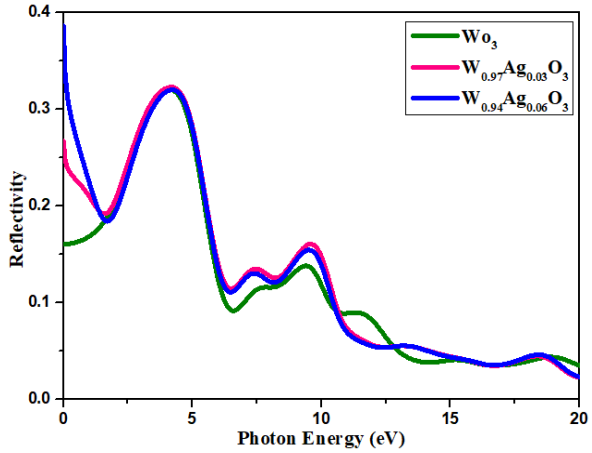


Figure 5: Reflectivity

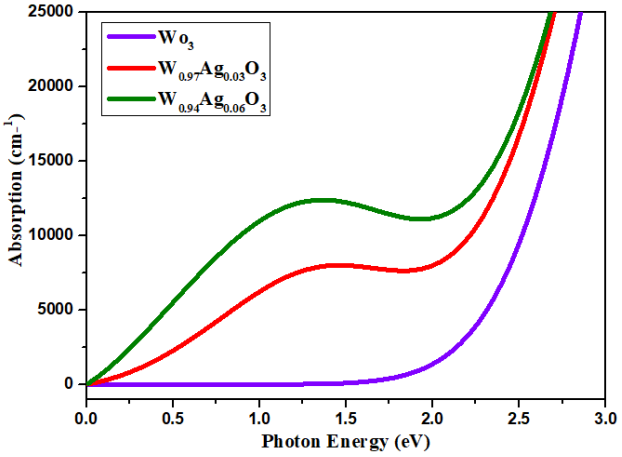


Figure 6: Absorption

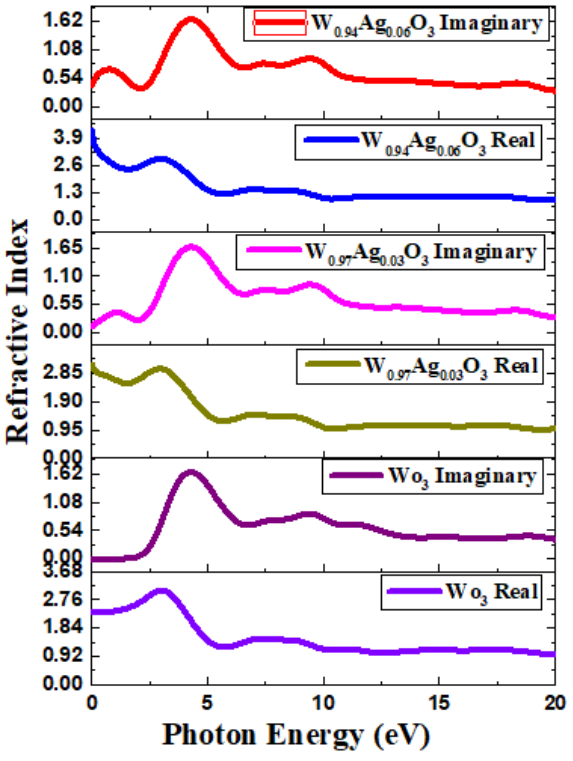


Figure 7: Refractive Index

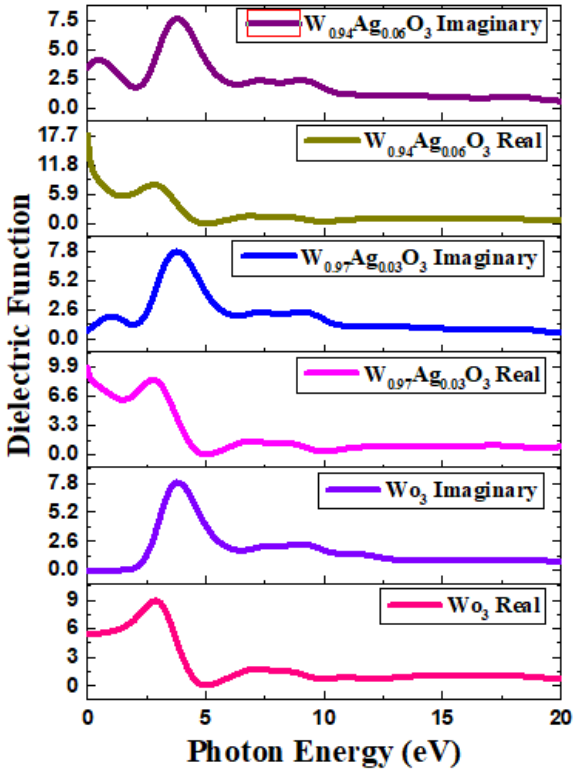


Figure 8: Dielectric Function

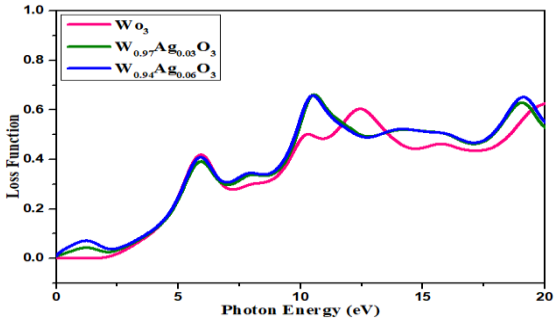


Figure 9: Loss Function

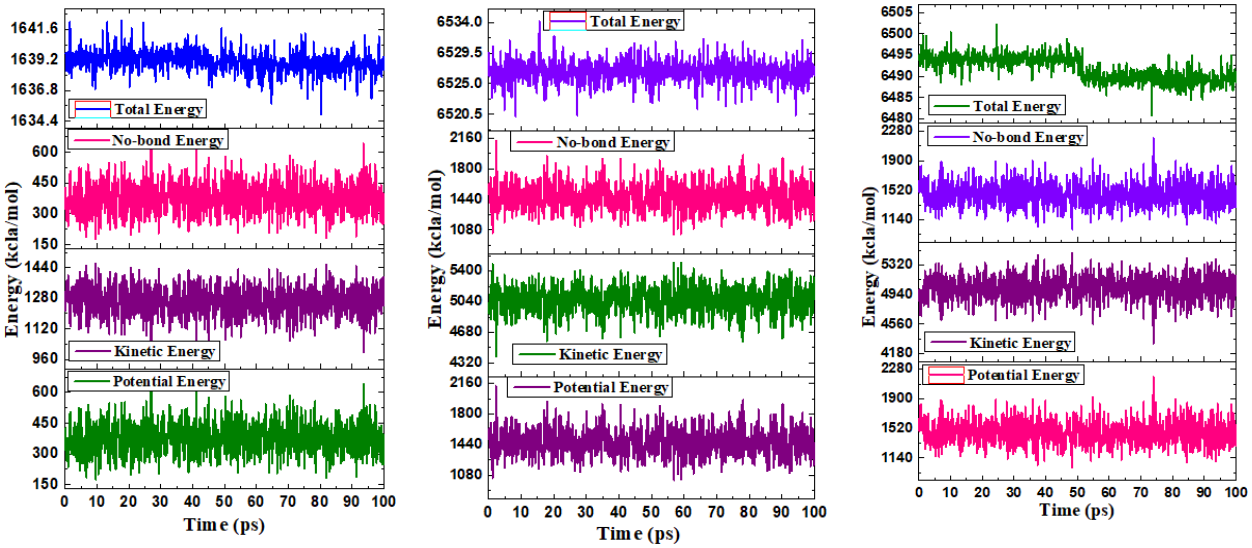


$WO_3$ $W0.97Ag0.03O_3$ $W_{0.94}Ag_{0.06}O_3$

## 4. Conclusion

Decreasing the electronic band gap by doping the Ag atom with $WO_3$ –leading to the augment of absorption rate of visible light or UV light in wastewater—is the ultimate goal of our research. From the functional of GGA with PBE, the calculated electronic structures of $WO_3$, $W_{0.97}Ag_{0.03}O_3$, and $W_{0.94}Ag_{0.06}O_3$ crystals are 2.031 eV, 0.227 eV and 0.171 eV, respectively. From the comparison of band gap, it can be said that the band gap has reduced with increasing the Ag doping in $WO_3$. Moreover, DOS can show how individuals' atom their contribution in TDOS and PDOS. In the section of optical properties, the absorption has increased in beginning photon energy by doping Ag atom with 3% and 6% that propounds the theoretical evidence to enhance the UV light absorption, and photocatalytic activity has grown up. The other underlying principle is found for the electronic and semiconductor devices in the area of materials science that $WO_3$ has been converted from semiconductor to superconductor by the little amount of Ag doping into the semiconductor, $WO_3$. The top-notch novelty has derived from the dynamic molecular study, which is related to total energy, kinetic energy, and potential energy into multifarious systems, and it undergoes the towering molecular disorder to show the highly activated state in photocatalytic reaction.

## 5. Funding

Author did not achieve any research fund from any institutions

## 6. References

[1]C.Y. Li, Siyu; Zhang, Xiaoxu; Wang, Yun; Liu, Chunbo; Chen, Gang; Dong, Hongjun, Insight into photocatalytic activity, universality and mechanism of copper/chlorine surface dual-doped graphitic carbon nitride for degrading various organic pollutants in water. Journal of colloid and interface science 538 (2019) 462-473.

[2]A. Ahmed Md Boshir; Ajoy Kumer; Islam Nazrul Muhammad; Islam Tajmeri Selima, The Photochemical Degradation (PCD) of Nitrobenzene (NB) using UV

Light and Fenton Reagent Under Various Conditions. Journal of the Turkish Chemical Society, Section A: Chemistry 5 (2018) 803-818.

[3]K. Ajoy, ; Md, Boshir Ahmed; Md Sharif, Arfat; Al-Mamun, Abdullah;, A Theoretical Study of Aniline and Nitrobenzene by Computational Overview. Asian journal of physical and chemical science 4 (2017) 1-12.

[4]U. Chakma, ; Kumer, Ajoy; Chakma, Kamal Bikash; Islam, Md Tawhidul ; Howlader, Debashis; Mohamed, Rasha M K;, Electronics structure and optical properties of $SrPbO_3$ and $SrPb_{0.94}Fe_{0.06}O_3$: A first principle approach. Eurasian Chemical Communications 2 (2020) 573-580.

[5]U. Chakma, ; Kumer, Ajoy; Chakma, Kamal Bikash; Islam, Md Tawhidul; Howlader, Debashis;, Electronics Structure and Optical Properties of $Ag_2BiO_3$,$(Ag_2)_{0.88}Fe_{0.12}BiO_3$: A First Principle Approach. Advanced Journal of Chemistry, Section A: Theoretical, Engineering and Applied Chemistry 3 (2020) 542–550.

[6]M.M. Hasan, Ajoy, Kumer, Chakma, Unesco;, Theoretical Investigation of Doping Effect of Fe for $SnWO_4$ in Electronic Structure and Optical Properties: DFT Based First Principle Study. Advanced Journal of Chemistry-Section A 03 (2020) 639–644.

[7]M.T. ISLAM, ; Ajoy, KUMER ; HOWLADER, Debashis; CHAKMA, Kamal Bikash;CHAKMA, Unesco;, Electronics structure and optical properties of $Mg(BiO_2)_4$ and $Mg(Bi_{0.91}Ge_{0.083}O_2)_4$: A first principle approach. Turkish Computational and Theoretical Chemistry 4 (2020) 24-31.

[8]B.C. Kamal, ;Ajoy, Kumer; Unesco, Chakma; Debashis, Howlade; Md Tawhidul, Islam;, A theoretical investigation for electronics structure of $Mg(BiO_2)_2$ semiconductor using first principle approach. International Journal of New Chemistry 7 (2020) 247-255.

[9]M.J. Islam, Ajoy, Kumer;, First-principles study of structural, electronic and optical properties of $AgSbO_3$ and $AgSb_{0.78}Se_{0.22}O_3$ photocatalyst. SN Applied Sciences 2 (2020) 251.

[10]K. Md. Mahmud Hasan; Ajoy, ; Unesco Chakma; and Md. Tawhidul Islam;, Structural, optical and electronic properties of $ZnAg_2GeTe_4$ and $ZnAg_2Ge_{0.93}Fe_{0.07}Te_4$ Photocatalyst: A first principle approach. Molecular Simulation 47 (2021) 1-13.

[11]S.U. MA Mokit, Chakma,; Ajoy Kumer,; Mohammad,Jahidul Islam, Ahsan Habib; Md Monsur Alam;, The Exploration of Structural, Electronic and Optical Properties for $MoS_2$ and $Mo_{0.95}W_{0.05}S_2$ Photocatalyst Effort on Wastewater Treatment using DFT Functional of First Principle Approach. Applied Journal of Environmental Engineering Science, 7 (2021) 103-113.

[12]C.D. Md Tawhidul Islam; Ajoy Kumer; Unesco, Howlader;, A Computational Investigation of Electronic Structure and Optical Properties of $AlCuO_2$ and $AlCu_{0.96}Fe_{0.04}O_2$: A First Principle Approach. Orbital: Electron. J. Chem 13 (2021).

[13]S.M. Karvinen, The effects of trace element doping on the optical properties and photocatalytic activity of nanostructured titanium dioxide. Industrial & engineering chemistry research 42 (2003) 1035-1043.

[14]M.M.A. Khan, Sajid A; Pradhan, D; Ansari, M Omaish; Lee, Jintae; Cho, Moo Hwan, Band gap engineered $TiO_2$ nanoparticles for visible light induced photoelectrochemical and photocatalytic studies. Journal of Materials Chemistry A 2 (2014) 637-644.

[15]N.B. Koriche, A; Aider, A; Trari, M, Photocatalytic hydrogen evolution over delafossite $CuAlO_2$. International Journal of Hydrogen Energy 30 (2005) 693-699.

[16]G.N. Li, Xin; Chen, Jiangyao; Jiang, Qi; An, Taicheng; Wong, Po Keung; Zhang, Haimin; Zhao, Huijun; Yamashita, Hiromi, Enhanced visible-light-driven photocatalytic inactivation of Escherichia coli using g-C3N4/TiO2 hybrid photocatalyst synthesized using a hydrothermal-calcination approach. Water research 86 (2015) 17-24.

[17]K.C. Li, Bo; Peng, Tianyou; Mao, Jin; Zan, Ling, Synthesis of multicomponent sulfide $Ag_2ZnSnS_4$ as an efficient photocatalyst for $H_2$ production under visible light irradiation. RSC Advances 3 (2013) 253-258.

[18]Y.p.F. Liu, Liang; Lu, Huidan; Liu, Laijun; Wang, Hai; Hu, Changzheng, Highly efficient and stable Ag/Ag3PO4 plasmonic photocatalyst in visible light. Catalysis Communications 17 (2012) 200-204.

[19]D.J.W.J.Z.S.N. Longhui;, $AgPO_4$/$Ag_2S$/g-$C_3N_4$ Preparation and performance of composite photocatalyst. Journal of Inorganic Chemistry 2019 (2019) 955-964.

[20]M.-Y.H. Lu, Meng-Hsiang; Ruan, Yen-Min; Lu, Ming-Pei, Probing the photovoltaic properties of Ga-doped CdS–Cu 2 S core–shell heterostructured nanowire devices. Chemical Communications 55 (2019) 5351-5354.

[21]X.D. Ma, Ying; Guo, Meng; Huang, Baibiao, The role of effective mass of carrier in the photocatalytic behavior of silver halide based Ag@ AgX (X= Cl, Br, I): A theoretical study. ChemPhysChem 13 (2012) 2304-2309.

[22]H.R.F. Mardani, Mehdi; Ziari, Mitra; Biparva, Pourya, Visible light photo-degradation of methylene blue over Fe or Cu promoted ZnO nanoparticles. Spectrochimica Acta Part A: Molecular and Biomolecular Spectroscopy 141 (2015) 27-33.

[23]A.L. Meng, Xiujuan; Wang, Xianlin; Li, Zhenjiang, Preparation, photocatalytic properties and mechanism of Fe or N-doped Ag/ZnO nanocomposites. Ceramics International 40 (2014) 9303-9309.

[24]T.O. Nakashima, Yoshihisa; Kubota, Yoshinobu; Fujishima, Akira, Photocatalytic decomposition of estrogens in aquatic environment by reciprocating immersion of $TiO_2$ modified polytetrafluoroethylene mesh sheets. Journal of Photochemistry and Photobiology A: Chemistry 160 (2003) 115-120.

[25]E.A. Romero, Ramunas; Novoderezhkin, Vladimir I; Ferretti, Marco; Thieme, Jos; Zigmantas, Donatas; Van Grondelle, Rienk, Quantum coherence in photosynthesis for efficient solar-energy conversion. Nature physics 10 (2014) 676.

[26]S.N. Sakthivel, B; Shankar, MV; Arabindoo, B; Palanichamy, M; Murugesan, V;, Solar photocatalytic

degradation of azo dye: comparison of photocatalytic efficiency of ZnO and TiO2. Solar energy materials and solar cells 77 (2003) 65-82.

[27]C.-C.N. Hu, Jun-Nan; Teng, Hsisheng;, Electrodeposited p-type Cu2O as photocatalyst for H2 evolution from water reduction in the presence of WO3. Solar energy materials and solar cells 92 (2008) 1071-1076.

[28]K.I. Tennakone, OA; Bandara, JMS; Kiridena, WCB;, $TiO_2$ and $WO_3$ semiconductor particles in contact: photochemical reduction of $WO_3$ to the non-stoichiometric blue form. Semiconductor science and technology 7 (1992) 423.

[29]T.Y. Arai, Masatoshi; Konishi, Yoshinari; Iwasaki, Yasukazu; Sugihara, Hideki; Sayama, Kazuhiro, Efficient complete oxidation of acetaldehyde into $CO_2$ over $CuBi_2O_4/WO_3$ composite photocatalyst under visible and UV light irradiation. The Journal of Physical Chemistry C 111 (2007) 7574-7577.

[30]B.G. Ma, Jianfeng; Dai, Wei-Lin; Fan, Kangnian, Ag-AgCl/$WO_3$ hollow sphere with flower-like structure and superior visible photocatalytic activity. Applied Catalysis B: Environmental 123 (2012) 193-199.

[31]G.H. Li, Jingjing; Zhang, Wenlei; Li, Pengwei; Liu, Guohua; Wang, Yingge; Wang, Kaiying, Graphene-bridged $WO_3/MoS_2$ Z-scheme photocatalyst for enhanced photodegradation under visible light irradiation. Materials Chemistry and Physics 246 (2020) 122827.

[32]C.C. Castillo, G; Chornik, B; Huentupil, Y; Buono-Core, GE, Characterization of photochemically grown Pd loaded $WO_3$ thin films and its evaluation as ammonia gas sensor. Journal of Alloys and Compounds 825 (2020) 154166.

[33]A.O. Navarro-Aguilar, S; Sanchez-Martinez, D; Hernández-Uresti, DB, An efficient and stable $WO_3$/g-$C_3N_4$ photocatalyst for ciprofloxacin and orange G degradation. Journal of Photochemistry and Photobiology A: Chemistry 384 (2019) 112010.

[34]Z.-Y.W. Liang, Jin-Xin; Wang, Xiu; Yu, Yan; Xiao, Fang-Xing, Elegant Z-scheme-dictated gC 3 N 4 enwrapped $WO_3$ superstructures: a multifarious platform for versatile photoredox catalysis. Journal of Materials Chemistry A 5 (2017) 15601-15612.

[35]S.J.S. Clark, M. D.; Pickard, C. J.; Hasnip, P. J.; Probert, M. J.; Refson, K.; Payne, M. C.;, "First principles methods using CASTEP. Zeitschrift fuer Kristallographie 220 (2005) 567-570.

[36]M. Segall, D; Lindan, Philip J., D.; Probert, M., J. al; Pickard, Christopher James; Hasnip, Philip James; Clark, SJ; Payne, M., C.,, First-principles simulation: ideas, illustrations and the CASTEP code. Journal of Physics: Condensed Matter 14 (2002) 2717.

[37]J. Ramos, Introducción a Materials Studio en la Investigación Química y Ciencias de los Materiales. (2020).

[38]E.H.P.C.a.W. Ouweltjes, Heats of formation of $Ag_3PO_4$ and $Ag_3AsO_4$. RECUEIL 90 (1971) 1343-1344.

[39]A.K. Vorontsov, EN; Balikhin, IL; Kurkin, EN ; Troitskii, VN ;Smirniotis, PG, Correlation of surface area with photocatalytic activity of TiO2. Journal of Advanced Oxidation Technologies 21 (2018) 20170063.